Inorg. Chem. **2002**, *41*, 1254–1262

Charge-Transfer Studies of Iron Cyano Compounds Bound to Nanocrystalline TiO_2 Surfaces

Mei Yang,[†] David W. Thompson,*[,‡] and Gerald J. Meyer*[,†]

Departments of Chemistry, Memorial University of Newfoundland, St. John's, Newfoundland, Canada A1B 3X7, and Johns Hopkins University, Baltimore, Maryland 21218

Received October 15, 2001

Nanocrystalline (anatase) titanium dioxide films have been sensitized to visible light with $K_4[Fe(CN)_6]$ and $Na_2[Fe(LL)(CN)_4]$, where LL = bpy (2,2′-bipyridine), dmb (4,4′-dimethyl-2,2′-bipyridine), or dpb (4,4′-diphenyl-2,2′-bipyridine). Coordination of $Fe(CN)_6^{4-}$ to the TiO_2 surface results in the appearance of a broad absorption band (fwhm ∼ 8200 cm^{-1}) centered at 23800 ± 400 cm^{-1} assigned to an Fe(II) → TiO_2 metal-to-particle charge-transfer (MPCT) band. The absorption spectra of $Fe(LL)(CN)_4^{2-}$ compounds anchored to TiO_2 are well modeled by a sum of metal-to-ligand charge-transfer (MLCT) bands and a MPCT band. Pulsed light excitation (417 or 532 nm, ∼8 ns fwhm, ∼2–15 mJ/pulse) results in the immediate appearance of absorption difference spectra assigned to an interfacial charge separated state [$TiO_2(e^-)$, Fe^{III}], $k_{inj} > 10^8$ s^{-1}. Charge recombination is well described by a second-order equal concentration kinetic model and requires milliseconds for completion. A model is proposed wherein sensitization of $Fe(LL)(CN)_4^{2-}/TiO_2$ occurs by MPCT and MLCT pathways, the quantum yield for the latter being dependent on environment. The solvatochromism of the materials allows the reorganization energies associated with charge transfer to be quantified. The photocurrent efficiencies of the sensitized materials are also reported.

Introduction

Dye sensitization of semiconductors is an attractive molecular approach for the conversion of light into electricity.[1] Sensitization of n-type semiconductors to visible light with metal cyano coordination compounds has been accomplished by two distinct mechanisms. In the first mechanism, termed *metal-to-particle charge-transfer* (MPCT) sensitization, light absorption promotes an electron localized in the metal center of the sensitizer directly to TiO_2 semiconductor, eq 1,

$$S/TiO_2 \xrightarrow{h\nu} S^+/TiO_2(e^-) \quad (1)$$

where S represents a sensitizer. In the second mechanism, termed metal-to-ligand charge-transfer (MLCT) sensitization, light absorption creates an MLCT excited state that then injects an electron to the semiconductor, eq 2.

$$S/TiO_2 \xrightarrow{h\nu} S^*/TiO_2 \xrightarrow{k_{inj}} S^+/TiO_2(e^-) \quad (2)$$

In either case, the electron may transfer to localized surface sites or to the delocalized conduction band of the semiconductor.

MPCT sensitization is mechanistically less complex as each absorbed photon is converted to an interfacial charge separated state, while the quantum yield for MLCT excited state electron transfer is known to depend upon a number of variables, such as the temperature,[2] the sensitizer excited state reduction potential,[3] the electrolyte ionic strength,[4] the solution and surface pH,[5] the applied potential,[6] and the excitation wavelength.[7] Nevertheless, the excited state electron transfer pathway has provided the most encouraging properties for practical solar cell applications,[8] and direct

* Authors to whom correspondence should be addressed. E-mail: meyer@jhuvms.hcf.jhu.edu (G.J.M.).
† Johns Hopkins University.
‡ Memorial University of Newfoundland.

(1) (a) Hagfeldt, A.; Grätzel, M. *Chem. Rev.* **1995**, *95*, 49. (b) Qu, P.; Meyer, G. J. In *Electron Transfer in Chemistry*; Balzani, V., Ed.; Wiley-VCH: Weinheim, 2001; Vol. 4, p 353.
(2) Qu, P.; Thompson, D. W.; Meyer, G. J. *Langmuir* **2000**, *16*, 4662.
(3) Argazzi, R.; Bignozzi, C. A.; Heimer, T. A.; Castellano, F. N.; Meyer, G. J. *Inorg. Chem.* **1994**, *33*, 5741.
(4) Kelly, C. A.; Farzad, F.; Thompson, D. W.; Stipkala, J. M.; Meyer, G. J. *Langmuir* **1999**, *15*, 7047.
(5) (a) Clark, W. D. K.; Sutin, N. *J. Am. Chem. Soc.* **1977**, *99*, 4676. (b) Sonntag, L. P.; Spitler, M. T. *J. Phys. Chem.* **1985**, *89*, 1453. (c) Qu, P.; Meyer, G. J. *Langmuir* **2001**, *17*, 6720.
(6) (a) O'Regan, B.; Moser, J.; Anderson, M.; Grätzel, M. *J. Phys. Chem.* **1990**, *94*, 8720. (b) Farzad, F.; Thompson, D. W.; Kelly, C. A.; Meyer, G. J. *J. Am. Chem. Soc.* **1999**, *121*, 5577.
(7) Moser, J.; Grätzel, M. *Chimia* **1998**, *52*, 160.

10.1021/ic011069q CCC: $22.00
Published on Web 02/14/2002

charge transfer has been used mainly for mechanistic studies of interfacial electron transfer.[9−13]

About 10 years ago it was shown that when metal cyanides, such as ferrocyanide, $Fe(CN)_6^{4-}$, bind to TiO_2 through the ambidentate cyano ligands, charge transfer bands appear in the visible region.[9] These bands were assigned as MPCT, $M^{n+}-CN-Ti(IV) \rightarrow M^{(n+1)+}-CN-Ti(III)$, where M = W, Fe, Mo, Ru, Re, or Os, and there is now considerable experimental evidence that supports this assignment.[9−12] More recently, sensitization of the same semiconductor following excitation of MLCT absorption bands in an Fe(II) polypyridyl cyano compound was realized.[14] A molecular compound, $Na_2[Fe(bpy)(CN)_4]$, where bpy is 2,2′-bipyridine, designed to sensitize semiconductors to visible light by *both* MPCT and MLCT pathways was recently reported.[12] By incorporating two charge transfer pathways into the semiconductor from one compound, broad spectral sensitization may be realized for solar energy conversion applications. In addition, since these two sensitization pathways have unique dynamics and can be initiated with different frequencies of light, the time-dependent optoelectronic responses can be precisely controlled and fine-tuned at the molecular level for other applications.

Here we present a more detailed analysis of the dual charge transfer pathways that expands upon the previous communication.[12] Two new iron sensitizers are reported, and their behavior on TiO_2 is contrasted with that of $Na_2[Fe(bpy)(CN)_4]$ and ferrocyanide. The solvatochromic properties of the compounds have been quantified to estimate reorganizational parameters and the solvation environment of the surface-bound compounds.

Experimental Section

Materials. Reagents. HPLC grade nitric acid, 70%, was obtained from Fisher Scientific. The $LiClO_4$, 99.99%, and tetrabutylammonium perchlorate ($TBAClO_4$), 99.99%, were obtained from Aldrich Chemical Company and used as received. Acetonitrile (Burdick and Jackson, spectroscopic grade) and tetrahydrofuran (Fisher, certified grade) were used as received. All other solvents were of reagent grade or better. The ligands were obtained from Aldrich and were used as received: 2,2′-bipyrdine (bpy) 99+%, 4,4-dimethyl-2,2′-bipyridine (dmb) 99%, and 4,4′-diphenyl-2,2′-bipyridine (dpb) tech. $K_4[Fe(CN)_6]$ was purchased from Aldrich.

Preparations. Coordination Compounds. The synthesis of $Na_2[Fe(bpy)(CN)_4]$ has previously been reported, and this procedure was extended to the other compounds by replacement of bpy with the appropriate ligand.[15a] ^1H NMR (CD_3OD) for $Na_2[Fe(bpy)(CN)_4]$: 7.24 (t, $J = 6$ Hz, 5, 5′ H); 7.72 (t, $J = 9$ Hz, 4, 4′ H); 8.09 (d, $J = 9$ Hz, 3, 3′ H); 9.56 (d, $J = 4$ Hz, 6, 6′ H). ^1H NMR (D_2O) for $Na_2[Fe(dmb)(CN)_4]$: 2.43 (s, 3H); 7.26 (d, $J = 7$ Hz, 5, 5′ H); 7.98 (s, 3, 3′ H); 9.04 (d, $J = 7$ Hz, 6, 6′ H). ^1H NMR (CD_3OD) for $Na_2[Fe(dpb)(CN)_4]$: 9.70 (d, $J = 6$ Hz), 8.65 (s), 7.93 (d, $J = 7$ Hz), 7.67 (d, $J = 6$ Hz), 7.5 (multiple, $J = 8$ Hz). Tetrabutylammonium, TBA, salts of $Fe(LL)(CN)_4^{2-}$ were obtained by ion exchange with an SP-Sephadex c-25 column.

Colloidal TiO_2 Films. TiO_2 films were prepared by a previously described sol−gel technique that produced mesoporous 10 μm thick film.[3] For absorption studies the films were coated onto glass slides rather than conductive glass. The glass slides were cut from plain microscope slides, VWR 25 × 75 × 1 mm, to ca. 12.5 × 50 mm, allowing the slides to be inserted diagonally into a 10 × 10 mm optical path length, quartz fluorescence cuvette. The thin films had dimensions of 12.5 mm × 15 mm × 10 μm. For infrared studies, the films were coated on the unpolished surface of CaF_2 windows (25 × 12 × 3 mm) purchased from International Crystal Laboratories.

Homogeneous dark yellow $[Fe(CN)_6]^{4-}$ derivatized TiO_2 films were formed by soaking the TiO_2 films in aqueous pH 2 solutions that contained 200 mM $K_4[Fe(CN)_6]$ for at least 4 h. $Na_2[Fe(LL)(CN)_4]$ was bound to the nanocrystalline TiO_2 surface after soaking in 0.5 mM ethanol solutions overnight. In the absorption isotherm studies, the solution concentration was varied and the surface concentration was determined by UV−vis spectroscopy.

Spectroscopy. UV−Vis Spectroscopy. All UV−visible absorption spectra were acquired at ambient temperature in air using a Hewlett-Packard 8453 diode array spectrometer. For sensitized films, the optical measurements were acquired by placing the TiO_2 on glass films diagonally in a solvent-filled 10 mm × 10 mm quartz cuvette, equipped with a 24/40 ground quartz joint. The cell was closed with a PTFE stopper and purged with argon through a needle. An unsensitized TiO_2 film was used as the reference.

NMR. ^1H NMR were obtained on a Bruker 300AMX FT-NMR spectrometer.

IR. Infrared measurements were made on a Perkin-Elmer Spectrum RX I Fourier transform IR spectrometer with a resolution of 2 cm^{-1}. IR of the free sensitizers was performed in standard KBr pellets. For sensitizers on TiO_2, measurements were made on a CaF_2 crystal in transmission mode with unsensitized CaF_2/TiO_2 as reference.

Transient Absorption. Transient absorption data were acquired as previously described with an ∼8 ns, 532 nm laser pulse from a Surelite II Nd:YAG, Q-switched laser or a 417 nm laser pulse, from a H_2-filled Raman shifter, for excitation and a pulsed 150 W Xe lamp as the probe source.[3] The excitation beam was ∼1 cm^2 and was attenuated to ∼2−15 mJ/pulse with a polarizer to avoid 2-photon excitation. Electron injection yields were determined by comparative actinometry as previously described.[4]

Electrochemistry. A PAR model 173 potentiostat/galvanostat was used in a standard three-electrode arrangement consisting of a Pt working electrode, a Pt gauze counter electrode, and a Ag/AgCl reference electrode. For fluid solution studies, approximately millimolar concentrations of the compounds were dissolved in the electrolyte. For surface studies, the sensitized TiO_2 material was used as the working electrode. The sensitized TiO_2 film was placed

(8) (a) O'Regan, B.; Grätzel, M. *Nature* **1991**, *353*, 737. (b) Nazeeruddin, M. K.; Kay, A.; Rodicio, I.; Humphry-Baker, R.; Mueller, E.; Liska, P.; Vlachopoulos, N.; Grätzel, M. *J. Am. Chem. Soc*. **1993**, *115*, 6382.
(9) (a) Vrachnou, E.; Vlachopoulos, N.; Grätzel, M. *J. Chem. Soc., Chem. Commun*. **1987**, *12*, 868. (b) Desilvestro, J.; Pons, S.; Vrachnou, E.; Grätzel, M. *J. Electroanal. Chem. Interfacial Electrochem*. **1988**, *246*, 411.
(10) (a) Lu, H.; Prieskorn, J. N.; Hupp, J. T. *J. Am. Chem. Soc*. **1993**, *115*, 5, 4927. (b) Blackbourn, R. L.; Johnson, C. S.; Hupp, J. T. *J. Am. Chem. Soc*. **1991**, *113*, 1060.
(11) (a) Ghosh, H. N.; Asbury, J. B.; Weng, Y.; Lian, T. *J. Phys. Chem. B* **1998**, *102*, 10208. (b) Weng, Y. X.; Wang, Y. Q.; Asbury, J. B.; Ghosh, H. N.; Lian, T. *J. Phys. Chem. B* **2000**, *104*, 93.
(12) Yang, M.; Thompson, D. W.; Meyer, G. J. *Inorg. Chem*. **2000**, *39*, 3738.
(13) Watson, D. F.; Bocarsly, A. B. *J. Phys. Chem. B* **2000**, *104*, 10909.
(14) (a) Ferrere, S.; Gregg, B. A. *J. Am. Chem. Soc*. **1998**, *120*, 843. (b) Ferrere, S. *Chem. Mater*. **2000**, *12*, 1083.
(15) (a) Schilt, A. *J. Am. Chem. Soc*. **1960**, *82*, 3000. (b) Toma, H. E.; Takasugi, M. S. *J. Solution Chem*. **1983**, 3470. (c) García Posse, M. E.; Katz, N. E.; Baraldo, L. M.; Poloneur, D. D.; Colombano, C. G.; Olabe, J. A. *Inorg. Chem*. **1995**, *34*, 1830. (d) Timpson, C. J.; Bignozzi, C. A.; Sullivan, B. P.; Kober, E. M.; Meyer, T. J. *J. Phys. Chem*. **1996**, *100*, 295.

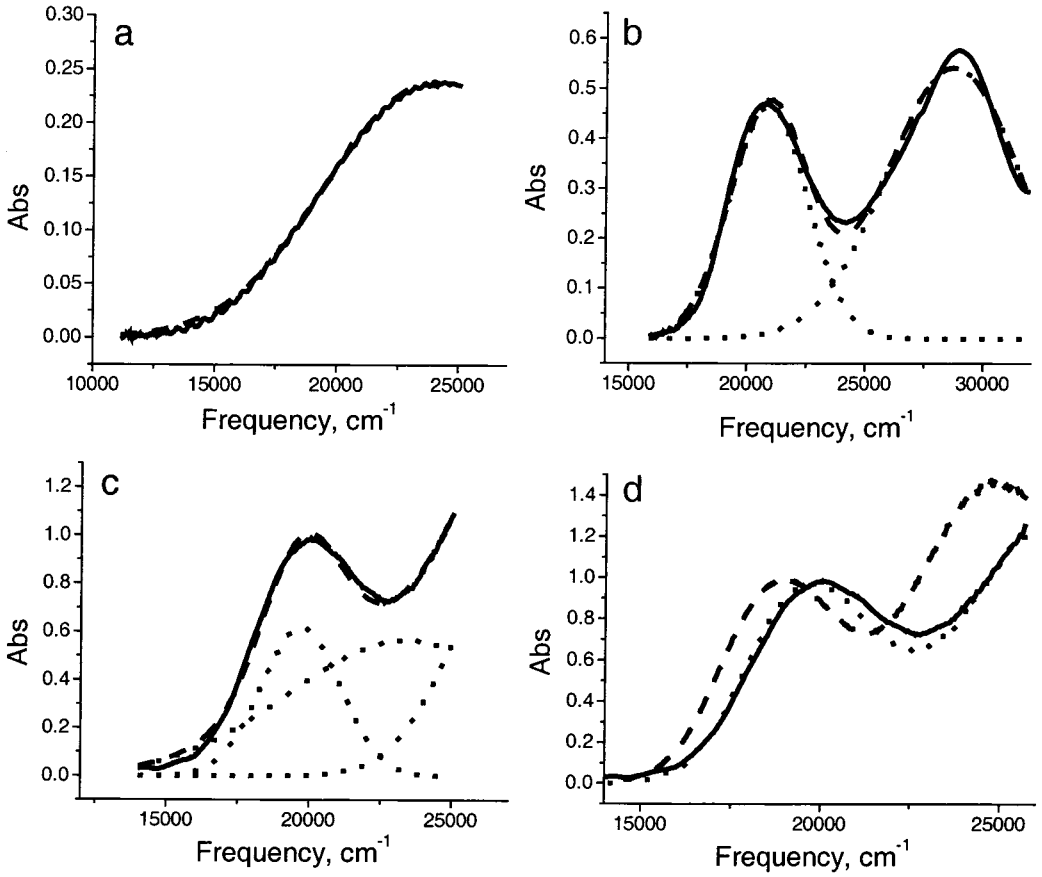

Figure 1. The visible absorption spectrum of (a) $Fe(CN)_6^{4-}/TiO_2$ in acetonitrile, (b) $Na_2Fe(bpy)(CN)_4$ in water, (c) $Fe(bpy)(CN)_4^{2-}/TiO_2$ in acetonitrile, and (d) $Fe(bpy)(CN)_4^{2-}/TiO_2$ (solid line), $Fe(dmb)(CN)_4^{2-}/TiO_2$ (dotted line), and $Fe(dpb)(CN)_4^{2-}/TiO_2$ (dashed line) in acetonitrile. Superimposed on the data are the results of spectral fitting to Gaussian absorption bands. See the Results section for more details.

under vacuum (~3 mmHg) for 3−4 h prior to electrochemical measurements.

Photoelectrochemistry. Photoelectrochemical and incident-photon-to-current efficiency (IPCE) measurements were performed in a two-electrode sandwich cell arrangement as previously described.[3] Briefly, ~10 μL of electrolyte was sandwiched between a TiO_2 electrode and a Pt coated tin oxide electrode. The supporting electrolyte was LiI/I_2 in acetonitrile. TiO_2 was illuminated with a 450 W Xe lamp coupled to an *f*/0.22 m monochromator. Photocurrents and voltages were measured with a Keithly model 617 digital electrometer. Incident irradiances were measured with a calibrated silicon photodiode from UDT Technologies.

Results

Figure 1a shows a typical absorption spectrum of an $Fe(CN)_6^{4-}$ derivatized mesoporous nanocrystalline TiO_2 thin film, abbreviated $Fe(CN)_6^{4-}/TiO_2$, in acetonitrile. A broad absorption band with a maximum ~420 nm that extends beyond 600 nm is observed. Measurements at wavelengths of light less than 400 nm (>28000 cm^{-1}) were difficult to accurately obtain due to the strong fundamental absorption of TiO_2. The absorption spectrum of $Fe(CN)_6^{4-}/TiO_2$ films were measured at different $[Fe(CN)_6]^{4-}$ surface coverage that correspond to extremes in absorption maximum from 0.05 to 0.5. For all samples, the normalized spectra displayed the same maximum and full-width-at-half-maximum (fwhm) within experimental error. The concentration dependent equilibrium binding data were well described by the Langmuir absorption isotherm model from which adduct formation constants of 100 ± 30 M^{-1} were abstracted. There was no measurable change in the absorption spectrum of $Fe(CN)_6^{4-}/TiO_2$ when the $LiClO_4$ concentration was varied from 0.0 to 1.0 M in acetonitrile.

Figure 1b shows the aqueous $Na_2[Fe(bpy)(CN)_4]$ solution absorption spectrum with two Gaussian absorption bands and their sum overlaid. Figure 1c is the absorbance spectrum of $Fe(bpy)(CN)_4^{2-}/TiO_2$ in acetonitrile, and Figure 1d compares this absorption spectrum with those of $Fe(dmb)(CN)_4^{2-}/TiO_2$ and $Fe(dpb)(CN)_4^{2-}/TiO_2$. The $Fe(LL)(CN)_4^{2-}$ derivatized material, where LL is bpy, dmb, or dpb, displays a broad absorption band that blue shifts ~100 cm^{-1} and increases in intensity by about 10% with the addition of 0.5 M $LiClO_4$ to the acetonitrile bath.

The absorption spectra shown in Figure 1 have been simulated on the basis of Gaussian distributions of charge transfer bands. The absorbance spectra of $Fe(CN)_6^{4-}/TiO_2$ were well described by a single MPCT band. The absorption spectra of $Fe(LL)(CN)_4^{2-}/TiO_2$ were modeled assuming that (1) the energy separation between the two MLCT bands and their bandwidths observed in fluid solution are preserved at the surface; and (2) the MPCT band for $Fe(LL)(CN)_4^{2-}/TiO_2$ maintains the same fwhm as $Fe(CN)_6^{4-}/TiO_2$, but the maximum frequency is bathochromically shifted by an amount that corresponds to the difference in $Fe^{III/II}$ reduction potential between $Fe(CN)_6^{4-}/TiO_2$ and $Fe(LL)(CN)_4^{2-}/TiO_2$

Table 1. Electrochemical, Optical, and Reorganization Parameters of $Fe(LL)(CN)_4^{2-}$, $Fe(CN)_6^{4-}/TiO_2$, and $Fe(LL)(CN)_4^{2-}/TiO_2$ in Acetonitrile and Tetrahydrofuran

		E_{op},[a] nm (eV)	$E_{1/2}(Fe^{III/II})$,[b] V (ΔE_{pp}, mV)	ΔG,[c] eV	λ^{MLCT},[d] eV
$Fe(CN)_6^{4-}/TiO_2$	ACN	420 (2.95)	−0.14 (92)		
	THF	420 (2.95)	−0.23 (150)		
$[Fe(bpy)(CN)_4]^{2-}$	ACN	673 (1.84)	−0.62 100	1.74	0.10
	THF	680 (1.82)	−0.70 (81)	1.68	0.14
$[Fe(dmb)(CN)_4]^{2-}$	ACN	666 (1.86)	−0.64 (94)	1.82	0.04
	THF	671 (1.85)	−0.79 (135)	1.67	0.18
$[Fe(dpb)(CN)_4]^{2-}$	ACN	704 (1.76)	−0.61 (83)	1.69	0.07
	THF	708 (1.75)			
$Fe(bpy)(CN)_4^{2-}/TiO_2$	ACN	507 (2.44)	−0.19 (46)	2.17	0.32
	THF	528 (2.35)	−0.35 (65)	2.01	0.37
$Fe(dmb)(CN)_4^{2-}/TiO_2$	ACN	509 (2.44)	−0.27 (44)	2.19	0.25
	THF	530 (2.34)	−0.40 (76)	2.06	0.28
$Fe(dpb)(CN)_4^{2-}/TiO_2$	ACN	535 (2.35)	−0.24 (56)	2.06	0.29
	THF	560 (2.21)	−0.29 (60)	2.01	0.23

[a] In fluid solution, E_{op} corresponds to the measured absorbance maximum for the lower-energy MLCT band. For the surface-bound compounds, E_{op} corresponds to the MLCT maximum calculated by Gaussian deconvolution of the measured spectra. [b] $E_{1/2}$ for $Fe^{III/II}$ measured versus ferrocene. The values in parentheses are the peak-to-peak separation, ΔE_{pp}, in mV. [c] ΔG is the Gibbs free energy stored in the MLCT state. [d] λ^{MLCT} is the total reorganization energy for Fe → bpy′ charge transfer.

measured by cyclic voltammetry in the appropriate solvent. The MPCT-to-MLCT band intensity ratio and the MLCT absorption maximum were then optimized until the best fit was obtained.

The visible absorption spectra for $Fe(LL)(CN)_4^{2-}$ and $Fe(LL)(CN)_4^{2-}/TiO_2$ were found to be solvent dependent.[15] Table 1 shows the low-energy MLCT maxima, E_{op} measured in fluid solution and calculated by the Gaussian deconvolution procedure for the surface-bound compounds. Within experimental error of ±4 nm, the absorption spectra of $Fe(CN)_6^{4-}/TiO_2$ and unsensitized TiO_2 films were independent of the external solvent. The absorption spectra in dimethylformamide could not be studied in as much detail due to slow desorption of the iron compounds from the surface.

Shown in Figure 2a and Figure 2c are the FT-IR spectra of $K_4[Fe(CN)_6]$ and $Na_2[Fe(bpy)(CN)_4]$. The cyanide stretching frequency of $K_4[Fe(CN)_6]$ was found at 2045 cm^{-1}. The $Na_2[Fe(bpy)(CN)_4]$ spectrum displays four close-lying bands which are at 2030, 2045, 2062, and 2085 cm^{-1}, respectively.[18,19] Figure 2b and Figure 2d are the FT-IR spectra of the derivatized TiO_2 films. The $Fe(CN)_6^{4-}/TiO_2$ surface displays an intense and broad absorption band at 2049 cm^{-1}

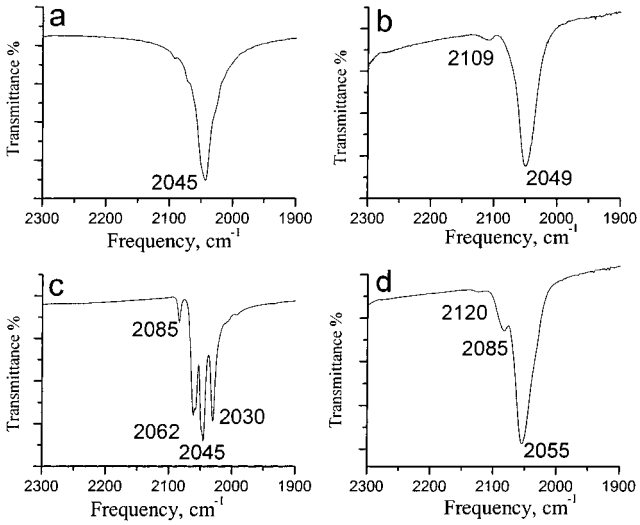

Figure 2. The infrared spectra of (a) $K_2Fe(CN)_6$ in a KBr pellet, (b) $Fe(CN)_6^{4-}/TiO_2$ deposited on CaF_2 window, (c) $Na_2Fe(bpy)(CN)_4$ in a KBr pellet, and (d) $Fe(bpy)(CN)_4^{2-}/TiO_2$ deposited on CaF_2 window. The spectra shown are averages of 32 scans with aresolution of 2 cm^{-1}.

and a weak band at 2109 cm^{-1}. The $Fe(bpy)(CN)_4^{2-}/TiO_2$ surface displays a broad band at 2055 cm^{-1} with a shoulder peak at 2085 cm^{-1} and a weak band at 2120 cm^{-1}.

Figure 3 shows the transient absorption spectra for $Fe(bpy)(CN)_4^{2-}/TiO_2$ in neat acetonitrile and with added 0.5 M $LiClO_4$ after pulsed 532 nm (~8 ns fwhm, ~12 mJ/pulse) light excitation. The magnitude of the absorption difference was typically two to three times larger in 0.5 M $LiClO_4$ compared to neat acetonitrile. The transient absorption spectra of $Fe(dmb)(CN)_4^{2-}/TiO_2$ and $Fe(dpb)(CN)_4^{2-}/TiO_2$ illustrated the same general features as $Fe(bpy)(CN)_4^{2-}/TiO_2$. However, the transient absorption spectra following pulsed excitation of $Fe(CN)_6^{4-}/TiO_2$ were unchanged by the addition of 0.5 M $LiClO_4$. Quantum yield measurements of $Fe(CN)_6^{4-}/TiO_2$ at 400 nm and $Fe(bpy)(CN)_4^{2-}/TiO_2$ at 500 nm resulted in a quantum yield of 0.8 ± 0.2 using an extinction coefficient of 5000 ± 200 M^{-1} cm^{-1} and 4200 ± 200 M^{-1} cm^{-1}, respectively. The recovery of the $Fe(bpy)(CN)_4^{2-}/TiO_2$ ground state absorption after pulsed light excitation was well fit to a second-order equal-concentration kinetic model over the first microsecond, $k_{obs} = 3 \pm 2 \times 10^9$ s^{-1}. The full recovery of the initial spectrum required milliseconds and was not quantified in detail.

The compounds display quasi-reversible $Fe^{III/II}$ redox chemistry by cyclic voltammetry in fluid solution and when anchored to nanocrystalline TiO_2 films. The redox chemistry is termed quasi-reversible because the anodic and cathodic currents are approximately equal but the peak-to-peak separation is nonzero for the surface-bound compounds at scan rates of 50−200 mV/s.[16] The surface-bound iron compounds were far more stable in the ferrous state than in the ferric state. Slow scan rates, <10 mV/s, or potential hold experiments positive of the $Fe^{III/II}$ reduction potential lead to significant desorption of the compounds. Attempts to directly bind $Fe^{III}(CN)_6^{3-}$ to the semiconductor surfaces were unsuccessful. The long-term instability of the ferric states on the nanocrystalline surface prevented the use of spectro-

(16) Bard, A. J.; Faulkner, L. R. *Electrochemical Methods: Fundamentals and Applications*; Wiley Interscience: New York, 1980.

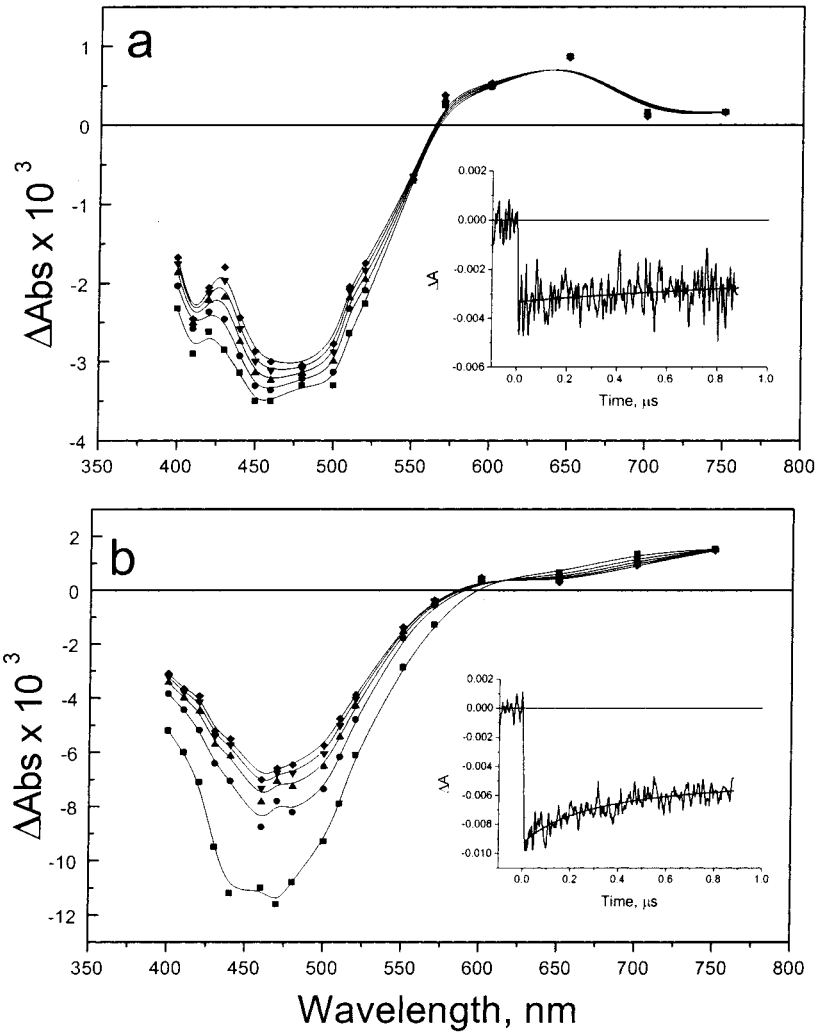

Figure 3. Transient absorption difference spectra of $Fe(bpy)(CN)_4^{2-}/TiO_2$ in (a) neat acetonitrile at delay times of (■) 0 μs, (●) 0.2 μs, (▲) 0.4 μs, (▼) 0.6 μs, and (◆) 0.8 μs and in (b) 0.5 M $LiClO_4$ acetonitrile recorded at delay times of (■) 0 μs, (●) 0.2 μs, (▲) 0.4 μs, (▼) 0.6 μs, and (◆) 0.8 μs. The insets in panels a and b are kinetic traces collected at 500 nm under the corresponding conditions. The samples were excited with a pulsed 532.5 nm light (12 mJ/pulse, fwhm 8 ns) at 25 °C under an argon atmosphere.

electrochemistry to quantify the absorption spectrum of the oxidized compounds and the possible appearance of outer-sphere intervalence transfer bands for mixed-valence surfaces, i.e., $Fe^{III}(CN)_6^{3-}$, $Fe^{II}(CN)_6^{4-}/TiO_2$.

Shown in Figure 4a are the photoaction spectra of the sensitized materials in a regenerative solar cell in 0.5 M LiI−0.05 M I_2 acetonitrile. Repetitive trials showed that the sensitized materials were stable and reproducible. No attempts were made to study the long-term (>hours) stability of the sensitized materials. The IPCE is the incident photon-to-current efficiency, which was calculated with eq 3. With-

$$\mathrm{IPCE} = \frac{(1240\ \mathrm{eV{\cdot}nm})(\text{photocurrent density}\ \mu\mathrm{A/cm^2})}{(\lambda\ \mathrm{nm})(\text{irradiance}\ \mu\mathrm{W/cm^2})} \quad (3)$$

out extensive optimization the IPCE maximum values were at most 13% and, for materials with the same ground-state absorption, followed the trend $Fe(bpy)(CN)_4^{2-}/TiO_2 > Fe(dpb)(CN)_4^{2-}/TiO_2 \geq Fe(dmb)(CN)_4^{2-}/TiO_2$.

Shown in Figure 4b are the absorptance ($1 - T$) spectrum of $Fe(bpy)(CN)_4^{2-}/TiO_2$ in 0.5 M $LiClO_4$ acetonitrile solution compared to the photoaction spectrum of $Fe(bpy)(CN)_4^{2-}/TiO_2$ in 0.5 M LiI−0.05 M I_2 acetonitrile electrolyte. The Gaussian modeling in Figure 1 indicates that MLCT and MPCT contributions to the observed absorption spectrum are approximately equal for the $Fe(LL)(CN)_4^{2-}/TiO_2$ materials. The photoaction spectrum shows that the MLCT contributions to the photocurrent are small relative to the MPCT contributions under all conditions studied.

Discussion

In a previous communication, we provided strong spectroscopic evidence that TiO_2 sensitization by $Fe(bpy)(CN)_4^{2-}$ occurs by a combination of two discrete pathways: $Fe^{II} \rightarrow bpy'$ (MLCT) and $Fe^{II} \rightarrow Ti^{IV}$ (MPCT) sensitization.[12] The evidence for the MLCT pathway was the observation of an efficient, ionic strength dependent, quantum yield for electron injection measured after excitation of the Fe → bpy charge transfer. The MPCT pathway gave the expected ionic strength independent injection quantum yield of unity. In regenerative solar cells with $Fe(bpy)(CN)_4^{2-}/TiO_2$, the direct charge transfer pathway was found to be more efficient than

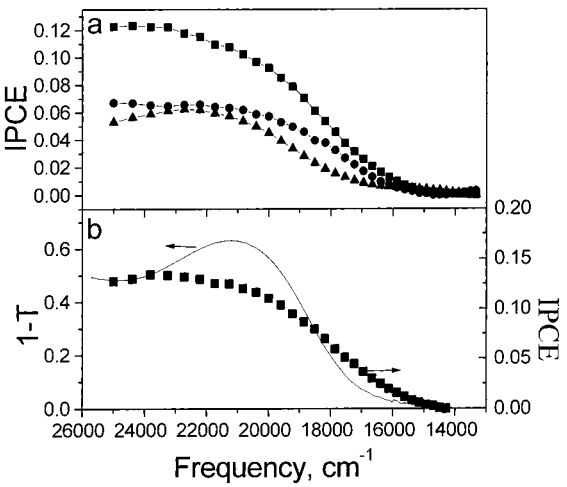

Figure 4. (a) Photoaction spectra of (■) $Fe(bpy)(CN)_4^{2-}/TiO_2$, (●) $Fe(dpb)(CN)_4^{2-}/TiO_2$, and (▲) $Fe(dmb)(CN)_4^{2-}/TiO_2$, obtained at room temperature in LiI/I_2 acetonitrile solutions. The IPCE is the incident-photon-to-current efficiency. Additional details are given in the text. (b) Comparison of $1 - T$ spectrum of $Fe(bpy)(CN)_4^{2-}/TiO_2$ in 0.5 M $LiClO_4$ acetonitrile to the photoaction spectrum of $Fe(bpy)(CN)_4^{2-}/TiO_2$ in 0.5 M LiI/0.05 M I_2 acetonitrile.

was the MLCT pathway. The results with the substituted bpy ligands, dmb and dpb, and additional solvent reported here support these previous findings.[12]

Although visible light absorption by $Fe(LL)(CN)_4^{2-}$ initially forms a ^{1}MLCT state, it is not clear that a MLCT state injects an electron into the semiconductor. Intramolecular excited state decay from the ^{1}MLCT state to form a ligand field excited state is known to be rapid for iron bipyridyl compounds in fluid solution.[17,18] With our temporal resolution all that can be safely stated is that MLCT absorption is the first step in the sensitization mechanism and that $k_{inj} > 10^8$ s^{-1}. We note that interfacial electron transfer from bipyridine ligands that are not bound to the semiconductor surface is known for MLCT excited states[2] but, to our knowledge, electron injection from ligand field states has not been observed.

Below we summarize new aspects of the surface coordination chemistry and the charge transfer reorganizational parameters that were extracted from the novel solvatochromic and redox properties of these sensitized materials.

Surface Coordination. The coordination of $Fe(CN)_6^{4-}$ to nanocrystalline TiO_2 leads to the appearance of a visible absorption band centered at 420 nm.[12] The absorption band has previously been observed for aqueous colloids and assigned to a MPCT band, Fe(II) → Ti(IV), shown as eq 4.

$$Fe^{II}-CN-|Ti^{IV} \xrightarrow{h\nu} Fe^{III}-CN-|Ti^{III} \qquad (4)$$

The broad absorption spectra of $Fe(LL)(CN)_4^{2-}/TiO_2$ are well modeled by a sum of MPCT and MLCT contributions.

The IR spectrum of $K_4Fe(CN)_6$ shows a band at 2045 cm^{-1}, assigned to the F_{1u} mode, while the spectrum of $Fe(LL)(CN)_4^{2-}$ displays the four ν(CN) modes $2A_1$, B_1, and B_2, expected for a C_{2v} symmetry.[19,20] Unfortunately, significant broadening precludes identification of the symmetry of the surface-bound compounds. However, the surface-bound complexes do display a weak band at higher energy, 2109 cm^{-1} for $Fe(CN)_6^{4-}/TiO_2$ and ∼2120 cm^{-1} for $Fe(LL)(CN)_4^{2-}/TiO_2$, not observed for the free compounds. These bands are reasonably assigned to bridging cyanide ligand(s). The shift to higher energy is consistent with previous studies.[10b,11] The lower frequency measured for the bridging CN ligand(s) in $Fe(CN)_6^{4-}/TiO_2$ relative to $Fe(LL)(CN)_4^{2-}/TiO_2$ suggests stronger σ-donation for $Fe(CN)_6^{4-}$. In the text, the surface coordination is abbreviated $Fe^{II}-CN-Ti^{IV}$; however, it should be kept in mind that there may be one, two, or even three cyanides bound to the TiO_2 surface.

Surface coordination has a profound impact on the $Fe^{III/II}$ reduction potentials of the iron compounds and induces a 200−500 mV anodic shift. In contrast, ruthenium sensitizers bound through dcb, where dcb is 4,4′-$(CO_2H)_2$-2,2′-bipyridine, ligands have $Ru^{III/II}$ reduction potentials that are within 50 mV of those measured in fluid acetonitrile electrolyte.[2,5c] In regenerative solar cells, with iron cyano sensitizers, this surface-induced potential shift decreases the spectral response of the materials at long wavelengths of light, but increases the driving force for iodide oxidation. The measured $Fe^{III/II}$ reduction potentials are considerably negative of the $Ru^{III/II}$ potentials in the widely used sensitizer *cis*-$Ru(dcb)_2(NCS)_2$, 0.85 V vs SCE.[8,21] Based on previous work, the low solar conversion efficiencies with all the iron sensitizers reported here likely stem from sluggish iodide oxidation rates that allow a significant fraction of the injected electrons to recombine with the oxidized iron compounds.[22]

Surface sites present on TiO_2 for coordination with the ambidentate cyano ligands are likely to be coordinatively unsaturated Ti^{IV} sites. The appearance of an absorption maximum for a MPCT band of $Fe(CN)_6^{4-}/TiO_2$ suggests that the acceptor is a Ti^{IV} state (d^0 electronic configuration) rather than a delocalized conduction band. In either case, however, the predominant electronic interaction would be σ-donation from the cyano nitrogen to the surface with insignificant π-back-bonding. This is consistent with the anodic shift in the $Fe^{III/II}$ reduction potential upon surface binding. The σ-donation should be less for the more Lewis acidic ferric state and may explain our inability to directly bind $Fe^{III}-$cyano compounds to the surface and our observations that the ferric compounds slowly desorb from the semiconductor surface during electrochemical measurements. We note that the adduct formation constants measured here for the ferrous cyano compounds are about 2 orders of magnitude lower than those reported for sensitizers bound through carboxylic acid groups.[2]

(17) Winkler, J. R.; Creutz, C.; Sutin N. *J. Am. Chem. Soc.* **1987**, *109*, 3470.
(18) (a) Creutz, C.; Chou, M.; Netzel, T. L.; Okumura, M.; Sutin, N. *J. Am. Chem. Soc.* **1980**, *102*, 309. (b) Sutin, N.; Creutz, C. *Pure Appl. Chem.* **1980**, *52*, 2717. (c) Sutin, N.; Creutz, C. *J. Chem. Educ.* **1983**, *60*, 809. (d) Winker, J. R.; Sutin, N. *Inorg. Chem.* **1987**, *26*, 220.
(19) (a) Umapathy, S.; MaQuillan, A. J.; Hester, R. E. *Chem. Phys. Lett.* **1990**, *170*, 128. (b) Korzeniewski, C.; Severson, M. W.; Schmidt, P. P.; Pons, S.; Fleischmann, M. *J. Phys. Chem.* **1987**, *91*, 5568.
(20) Schilt, A. A. *Inorg. Chem.* **1964**, *3*, 1323.
(21) Bond, A. M.; Deacon, G. B.; Howitt, J.; MacFarlane, D. R.; Spiccia, L.; Wolfbauer, G. *J. Electrochem. Soc.* **1999**, *146*, 648.
(22) Argazzi, R.; Bignozzi, C. A.; Heimer, T. A.; Hasselmann, G. M.; Meyer, G. J. *J. Phys. Chem B* **1998**, *102*, 7577.

Table 2. Intervalence Charge Transfer Parameters for $Fe(CN)_6^{4-}$ Ion Pairs, Mixed-Valence Compounds, and TiO_2 Interfacial Systems

complex	ν_{max}, nm (cm^{-1})	ϵ, M^{-1} cm^{-1}	$\Delta\nu_{1/2}$, cm^{-1}	f^c	μ_{12}, e Å	H_{DA}, cm^{-1}	ref
			Ion Pairs				
$Fe(CN)_6^{4-}/Fe(CN)_6^{3-}$	820 (12200)	28	7900	0.001	~0.09	44	24
$Fe(CN)_6^{4-}/Ru(NH_3)_6^{3+}$	730 (13660)	34	6300	0.001	~0.08		24
$Fe(CN)_6^{3-}/Os(CN)_6^{4-}$	610 (16400)	45	10100	0.002	~0.11	73	24
			Mixed-Valence Compounds				
$[(CN)_5Fe^{II}(\mu\text{-}CN)Fe^{III}(CN)_5]$	1300 (7700)	3200	4900	0.07			25
$[(CN)_5Fe^{II}(\mu\text{-}CN)Ru^{III}(NH_3)_5]^a$	820 (12200)		2860	0.08	0.77[b]	2800	26
$[(CN)_5Fe^{II}(\mu\text{-}CN)Os^{III}(NH_3)_5]^a$	561 (17800)	3600	3400	0.06	0.44[b]	2600	26
			TiO_2 Interfacial Systems				
$[(CN)_5Fe^{II}(\mu\text{-}CN)Ti^{IV}O_2]$	420 (23800)	5200	8200	0.2	~0.9	~3000	9
$[(CN)_3(bpy)Fe^{II}(\mu\text{-}CN)Ti^{IV}O_2]$	427 (23400)	5200	8200				*d*

[a] Measured at 77 K. [b] Determined from room temperature absorption spectra. [c] Calculated from eq 5 or 6. [d] This work.

An interesting observation is that the $Fe^{III/II}$ reduction potential of $Fe(CN)_6^{4-}/TiO_2$ is solvent dependent while the energy and spectral distribution of the MPCT band is not. For example, an ~90 mV shift of the $Fe^{III/II}$ reduction potential is observed when the solvent is changed from acetonitrile to THF while the MPCT bands in both solvents are superimposable. This indicates that the $Ti^{IV/III}$ reduction potential, or the energetic position of the conduction band, tracks the $Fe^{III/II}$ reduction potential and shifts in energy a corresponding amount. Precedence for such behavior exists from the work of Zaban and co-workers, who have shown that sensitizers with pH independent reduction potentials in fluid solution can become pH dependent when bound to nanocrystalline TiO_2 surfaces.[23] It therefore appears that the solvent interaction with TiO_2 indirectly influences the $Fe^{III/II}$ reduction potential. Additional details of the solvatochromic properties are given below.

Comparison with Known Intervalence Transfer (IT) Bands. Spectroscopic IT band maxima, extinction coefficients, and bandwidth parameters for ion pairs, mixed valence compounds, and TiO_2 interfacial systems that contain the $Fe(CN)_6$ moiety are given in Table 2. The values for the oscillator strength (f_{osc}), the transition dipole moment (μ_{12}), and the electronic coupling element (H_{DA}) for $Fe^{II}-CN-Ti^{IV}$, calculated with eqs 5−7, are also given in Table 2.[27]

Experimentally, the oscillator strength f_{osc} of a Gaussian charge transfer band is given by eq 5,[27]

$$f_{osc} = (4.61 \times 10^{-9})\epsilon_{max}\Delta\nu_{1/2} \quad (5)$$

where ϵ_{max} (M^{-1} cm^{-1}) and $\Delta\nu_{1/2}$ (M^{-1} cm^{-1}) are the extinction coefficient and full-width-at-half-maximum of the absorption band. The oscillator strength is related to the transition dipole moment by eq 6,[27]

$$f_{osc} = (8\pi^2 m_e c\nu_{max}/3he^2)|\mu_{12}|^2 = (1.08 \times 10^{-5})\nu_{max}|\mu_{12}|^2 \quad (6)$$

where ν_{max} is the energy at the band maxima in cm^{-1} and the transition dipole moment, μ_{12}, has units of e Å. The electronic coupling element H_{DA} may then be determined from eq 7,[27]

$$(H_{DA})^2 = (9.2 \times 10^4)(\nu_{max} f_{osc})/r_{DA}^2 \quad (7)$$

where r_{DA} (in Å) is the true charge transfer distance between the donor and the acceptor.[26] H_{DA} values for the D−CN−A compounds in Table 2 were calculated with r_{DA} values from Stark measurements as determined in the original references.[9,24−26] For the interfacial cases, models were used to crudely estimate a geometric value of $r_{DA} \sim 6$ Å.

Comparing the physical parameters given for the three classes of IT systems in Table 2, several striking features are apparent. The magnitude of $\Delta\nu_{1/2}$ is similar for the ion pairs and the interfacial TiO_2 systems, which are in turn much larger than those reported for the mixed-valence compounds. The oscillator strength for interfacial charge transfer is a factor of ~3 larger than that for the mixed-valence compounds and about 2 orders of magnitude larger than that reported for the ion pairs. The magnitude of the transition dipole moment is substantially lower for the ion pairs. The high oscillator strengths and large $\Delta\nu_{1/2}$ values for the interfacial compounds are advantageous for solar energy conversion applications where efficient and broad spectral harvesting of sunlight are generally required.

Evaluation of the oscillator strengths and the transition dipole moments does not require any assumptions. In contrast, the magnitude of the electronic coupling matrix element, H_{DA}, critically depends on the charge transfer distance assumed. As stated above, the true distance is not known and a geometric distance was assumed here. If charge transfer is to a delocalized conduction band, then the true r_{DA} may be larger, and it may be smaller if it is to a localized surface state. Therefore, a more precise value of r_{DA} is needed to accurately determine H_{DA}.

Reorganizational Parameters. A. Metal-to-Particle Charge Transfer. For mixed-valence compounds, the total reorganization energy for IT bands, and presumably MPCT bands, may be abstracted from the spectral data with the approach of Hush, eq 8,[28]

$$(\Delta\nu_{1/2})^2 = 16 \ln 2 k_B T\lambda^{MPCT} \quad (8)$$

(23) (a) Zaban, A.; Ferrere, S.; Sprague, J.; Gregg, B. A. *J. Phys. Chem. B* **1997**, *101*, 55. (b) Zaban, A.; Ferrere, S.; Gregg, B. A. *J. Phys. Chem. B* **1998**, *102*, 452.
(24) Billing, R.; Khoshtariya, D. E. *Inorg. Chem.* **1994**, *33*, 4038.
(25) McCartney, D. H. *Rev. Inorg. Chem.* **1994**, *33*, 4038.
(26) (a) Karki, L. Lu, H. P.; Hupp, J. T. *J. Phys. Chem.* **1996**, *100*, 15637. (b) Vance, F. W.; Karki, L.; Reigle, J. K.; Hupp, J. T.; Ratner, M. A. *J. Phys. Chem. A* **1998**, *102*, 8320.
(27) Creutz, C.; Newton. M. D.; Sutin, N. *J. Photochem. Photobiol., A: Chem.* **1994**, *82*, 47.

where k_B is the Boltzmann constant, T is temperature, and λ^{MPCT} is the total reorganization energy for MPCT. Applications of this relation to the data shown in Figure 1 yields a total reorganization energy of $\lambda^{MPCT} = 3.6$ eV for $Fe(CN)_6^{4-}/TiO_2$. This value seems unrealistically large, even if significant Jahn−Teller distortions for a $Ti^{IV/III}$ process are considered. Intuitively one might expect that inhomogeneous broadening could contribute to the large calculated reorganization energy. The electronic absorption spectra of $Fe(CN)_6^{4-}/TiO_2$ films measured as a function of $Fe(CN)_6^{4-}$ surface coverage in different solvents yielded the same $\Delta\nu_{1/2}$ within reasonable experimental error and provide no evidence for inhomogeneity. The broadened ν(CN) bands suggest that a distribution of sensitizer−semiconductor orientations are sampled on the vibrational time scale. In any case, extracting reorganization parameters directly from MPCT bands with Marcus−Hush theory does not appear to be adequate for these electron transfer processes. Estimates of λ^{MPCT} must be based on other experiments as discussed below.

The total reorganization energy for interfacial charge transfer, λ^{MPCT}, is the sum of the inner-sphere, λ_i^{MPCT}, and the outer-sphere, λ_o^{MPCT}, reorganization energies.[28] The inner-sphere contribution may be estimated from the resonance Raman data previously reported by Hupp and co-workers for $Fe(CN)_6^{4-}/TiO_2$ in H_2O.[10b] The mode-by-mode descriptions for inner-sphere reorganization from charge transfer excitation were obtained from the application of the time-dependent scattering theory to Raman spectra.[29] The inner-sphere reorganization energy is given by the sum of all the modes that are resonantly enhanced, eq 9,

$$\lambda_i^{MPCT} = 0.5\sum_k \Delta_k^2\left(\frac{\omega_k}{2\pi}\right) \quad (9)$$

where ω_k is the vibrational frequency multiplied by 2π and Δ_k is redox-induced normal coordinate displacements. Using Hupp's data with the assumption that all 10 enhanced modes contribute to the interfacial electron transfer, we calculate that λ_i^{MPCT} for $Fe(CN)_6^{4-}/TiO_2$ film is 2550 cm^{-1} (0.32 eV).[10b]

Estimation of the outer-sphere reorganization energy is more problematic. In principle, the solvent contributions may be estimated from the self-exchange rate constant, eq 10.

$$*Fe^{II}(CN)_6^{4-} + Fe^{III}(CN)_6^{3-} \xrightarrow{k_{11}} *Fe^{III}(CN)_6^{3-} + Fe^{II}(CN)_6^{4-} \quad (10)$$

Our attempts to measure this rate constant in situ were frustrated by the instability of the ferric compounds on the semiconductor surface. Literature values reported in fluid aqueous solution span an unusually large range, $\lambda_o^{MPCT} \sim 1700-7200$ cm^{-1} (0.2−0.9 eV).[30] Values for mixed-valence compounds with $Fe^{II}(CN)_6^{4-}$ donors are typically $\lambda_o^{IT} \sim 2200$ cm^{-1} (0.27 eV) and are probably better models for the interfacial case.[26] Use of these estimates from fluid aqueous solution ignores the influence of the semiconductor surface on the solvation of the iron compound. However, we find experimentally that the MPCT band is independent of the external solvent and is very similar to that reported for $Fe(CN)_6^{4-}/TiO_2$ aqueous colloids. Taken together, the spectroscopic observations suggest that the sensitizer is in a hydrated, aqueous-like layer and that outer-sphere contributions to λ_o^{MPCT} from the external solvent are minimal. Additional details on solvation energetics are available from the $Fe(LL)(CN)_4^{2-}/TiO_2$ data described further below.

If we take outer-sphere estimates from fluid aqueous solution and calculate λ_i^{MPCT} from the published Raman data for colloidal aqueous solutions, the total reorganization energy for the MPCT of $Fe(CN)_6^{4-}/TiO_2$ is ∼0.6 eV. For comparative purposes, the only reorganization parameters for electron injection available in the literature, to our knowledge, are those estimated for excited state sensitization of single-crystal electrodes in aqueous solution.[5] Despite gross differences in the mechanisms and molecular assemblies, the values are remarkably similar and within a factor of 2 of those estimated here, ∼0.3 eV.[5a,b]

B. MLCT Sensitization. The two broad visible absorption bands for $Fe(bpy)(CN)_4^{2-}$ have been assigned to Fe → bpy metal-to-ligand charge-transfer, MLCT.[17] The MLCT bands of metal polypyridyl cyano compounds, such as $Fe(bpy)(CN)_4^{2-}$, are known to be highly solvatochromic.[31] The change in dipole moment with light absorption and solvent interactions with the coordinated cyano ligand are thought to be the origin of the solvatochromism.[31] The solvatochromic MLCT absorption bands of $Fe(LL)(CN)_4^{2-}$ compounds bound to TiO_2 can thus serve as probes of interfacial solvation.

For the surface-bound compounds, the lower energy MLCT band is fully resolved while the fundamental absorption edge of TiO_2 completely obscures the high-energy MLCT band for $Fe(bpy)(CN)_4^{2-}$ and $Fe(dmb)(CN)_4^{2-}$ and partially obscures it for $Fe(dpb)(CN)_4^{2-}$. The blue shift in the MLCT absorption bands observed upon surface attachment are expected based on the CN → Ti^{IV} σ-donation, that decreases the electron density on iron, and an aqueous-like interface, Table 1.

In the classical limit, the optical energy for the long-wavelength MLCT band, E_{op}^{MLCT}, is related to the Gibbs free energy and the total reorganization energy of the MLCT excited state, eq 11,[31]

$$E_{op}^{MLCT} = \Delta G^{MLCT} + \lambda^{MLCT} \quad (11)$$

where ΔG^{MLCT} is well approximated by $E_{1/2}(Fe^{III/II}) - E_{1/2}(LL^{0/-})$. The metal-based reduction potentials have been measured for the surface-bound compounds directly by cyclic

(28) Hush, N. S. *Prog. Inorg. Chem.* **1967**, *8*, 391.
(29) (a) Heller, E. J.; Sundberg, R. L.: Tannor, D. *J. Phys. Chem.* **1982**, *86*, 1822. (b) Tannor, D. J.; Heller, E. J. *J. Chem. Phys.* **1982**, *77*, 202. (c) Lee, S. Y.; Heller, E. J. *J. Chem. Phys.* **1977**, *71*, 4777. (d) Heller, E. J. *Acc. Chem. Res.* **1981**, *14*, 368. (e) Morris, D E.; Woodruff, W. H. *J. Phys. Chem.* **1985**, *89*, 5795.
(30) (a) Campion, R. J.; Deck, C. F.; King, P.; Wahl, A. C. *Inorg. Chem.* **1976**, *6*, 672. (b) Terrettaz, S.; Becka, A. M.; Traub, M. J.; Fettinger, J. C.; Miller, C. J. *J. Phys. Chem.* **1995**, *99*, 11216.
(31) Chen, P. Y.; Meyer, T. J. *Chem. Rev.* **1998**, *98*, 1439.

voltammetry. The ligand reductions cannot be obtained experimentally because TiO_2 reduction occurs prior to the bipyridine reductions. However, studies by Curtis et al. for $Ru(bpy)(NH_3)_4^{2+}$ compounds have shown that the ligand-based reduction potentials are only weakly sensitive to solvent.[32] Assuming the same is true here, the electrochemical and optical data for the surface-bound compounds allow the direct determination of λ^{MLCT}. Shown in Table 1 are the reorganization energies calculated with eq 11.

The total reorganization energy for the surface-bound compounds is significantly larger than those in fluid solution for all three compounds studied in both acetonitrile and THF. This conclusion is demanded by the raw experimental data and is not an artifact of the Gaussian deconvolution or the assumptions made. In fact, if the observed absorption maximum were used rather than the calculated one, or if the ligand reduction potentials were allowed to shift in concert with the $Fe^{III/II}$ reduction potentials, the reorganization energy for the surface-bound compound would increase further. Therefore, while our data does not allow us to quantify the magnitude of the reorganization energy increase upon surface binding with high precision, the conclusion that it must increase is a near certainty.

The total reorganization energy for the MLCT excited state bound to the semiconductor surface is expected to include contributions from solution and the solid. The restricted translational mobility of the semiconductor-bound iron compounds and the external solvent probably underlie the enlarged reorganization energy relative to fluid solution. This work then demonstrates the influence of the TiO_2 semiconductor on the energetics of the MLCT state. Since the ground and ligand field states are expected to be perturbed by the semiconductor to a different degree, the results strongly suggest that the nonradiative decay pathways and lifetime of the MLCT state are also significantly influenced by the semiconductor interface.

(32) Chang, J. P.; Fung, E. Y.; Curtis, J. C. *Inorg. Chem.* **1986**, *25*, 4233.

Conclusions

Iron cyano compounds bound to nanocrystalline TiO_2 have allowed $Fe^{II} \rightarrow Ti^{IV}$ (MPCT) and $Fe^{II} \rightarrow bpy'$ (MLCT) charge transfer to be quantified by spectroscopic and electrochemical measurements. Surface binding alters the solution redox and optical properties of the iron compounds in a manner that can be rationally understood on the basis of the presence of ambidentate cyano ligands bound to the semiconductor surface. The MLCT bands were solvatochromic while the MPCT bands were not. The lack of solvatochromism for the MPCT bands, coupled with a significant change in the $Fe^{III/II}$ reduction potential measured electrochemically, suggests that the acceptor states in TiO_2 shift with solvent. Analysis of the solvatochromic MLCT bands demonstrated that the total excited state reorganization energy for $Fe \rightarrow bpy'$ charge transfer increased when the compounds were bound to the mesoporous nanocrystalline semiconductor film. This finding demonstrates that the excited state energetics, and presumably excited state relaxation processes, are profoundly impacted by coordination to semiconductor surfaces.

Acknowledgment. This work was supported by the National Science Foundation.

IC011069Q